An electrochemical immunosensor using *p*-aminophenol redox cycling by NADH on a self-assembled monolayer and ferrocene-modified Au electrodes

Seong Jung Kwon,[a] Haesik Yang,*[b] Kyungmin Jo[b] and Juhyoun Kwak*[a]

Received 15th April 2008, Accepted 24th June 2008
First published as an Advance Article on the web 11th August 2008
DOI: 10.1039/b806302h

Redox cycling of enzymatically amplified electroactive species has been widely employed for high signal amplification in electrochemical biosensors. However, gold (Au) electrodes are not generally suitable for redox cycling using a reducing (or oxidizing) agent because of the high background current caused by the redox reaction of the agent at highly electrocatalytic Au electrodes. Here we report a new redox cycling scheme, using nicotinamide adenine dinucleotide (NADH), which can be applied to Au electrodes. Importantly, *p*-aminophenol (AP) redox cycling by NADH is achieved in the absence of diaphorase enzyme. The Au electrodes are modified with a mixed self-assembled monolayer of mercaptododecanoic acid and mercaptoundecanol, and a partially ferrocenyl-tethered dendrimer layer. The self-assembled monolayer of long thiol molecules significantly decreases the background current of the modified Au electrodes, and the ferrocene modification facilitates easy oxidation of AP. The low amount of ferrocene on the Au electrodes minimizes ferrocene-mediated oxidation of NADH. In sandwich-type electrochemical immunosensors for mouse immunoglobulin G (IgG), an alkaline phosphatase label converts *p*-aminophenylphosphate (APP) into electroactive AP. The amplified AP is oxidized to *p*-quinoneimine (QI) by electrochemically generated ferrocenium ion. NADH reduces QI back to AP, which can be re-oxidized. This redox cycling enables a low detection limit for mouse IgG (1 pg mL^{-1}) to be obtained.

Introduction

Signal amplification is the most important strategy in lowering the detection limits of immunosensors,[1–3] and labels that can generate many signaling molecules per biospecifically-bound target have been widely used. Thus, signal-amplification methods with different types of labels, including a bio-barcode assay using Au nanoparticles[4,5] and a liposome-PCR assay using DNA-containing liposomes,[6] have been developed. However, enzymes are still more commonly used as labels for signal amplification[7–10] because of their high turnover frequencies and high reaction selectivity.[11,12]

To achieve higher signal amplification in electrochemical immunosensors, the enzymatic amplification step has been combined with a further amplification step, like the redox cycling of enzymatically amplified electroactive species. In redox cycling, electrochemically oxidized (or reduced) species are reduced (or oxidized) electrochemically,[13] enzymatically,[14,15] or chemically.[16–18] Thus, regenerated electroactive species are electrochemically re-oxidized (or re-reduced), resulting in high electrochemical signals. Generally, an additional electrode[19,20] or enzyme[21–23] has been used to achieve higher redox cycling. Recently, we have shown that hydrazine and sodium borohydride can be used for *p*-aminophenol (AP) redox cycling.[24,25] This type of redox cycling by chemical facilitates the simple but highly sensitive electrochemical detection of proteins without the need to use two electrodes or two enzymes. However, it requires strong reducing (or oxidizing) agents to ensure rapid chemical reaction. Strong reducing (or oxidizing) agents may be easily oxidized (or reduced) electrochemically at low potentials, which causes high background currents in electrochemical detection.[24,25] Thus, the redox reaction of such reducing (or oxidizing) agents should be very slow at electrodes, whereas their chemical reaction with electrochemically oxidized (or reduced) species should be very fast. This requirement could limit the use of highly electrocatalytic noble metal electrodes, such as gold (Au) electrodes.

The reduced form of nicotinamide adenine dinucleotide (NADH) has been widely used in AP redox cycling by diaphorase enzyme.[26,27] NADH converts oxidized diaphorase to a reduced form during redox cycling. The redox potential of the $NADH/NAD^+$ couple is –0.32 V *vs.* SHE at pH 7, indicating that NADH can act as a good reducing agent. Interestingly, the electrochemical oxidation of NADH requires high overpotentials at noble metal electrodes,[28–30] while the chemical reaction between diaphorase and NADH is very fast.[31] The slow electrochemical oxidation and fast chemical reaction of NADH enables its use in AP redox cycling by diaphorase at Au electrodes. On the other hand, NADH may reduce *p*-quinoneimine (QI) to AP in the absence of diaphorase,

[a]*Department of Chemistry, Korea Advanced Institute of Science and Technology (KAIST), Daejeon, Korea. E-mail: Juhyoun_Kwak@kaist.ac.kr; Fax: +82 42 350 2810; Tel: +82 42 350 2833*
[b]*Department of Chemistry, Pusan National University, Busan, Korea. E-mail: hyang@pusan.ac.kr*

suggesting that AP redox cycling by NADH might also be possible without diaphorase. However, there has been no report of redox cycling by NADH in biosensors.

Bare Au electrodes exhibit high and potential-dependent background currents in aqueous solutions because of their highly electrocatalytic properties, high charging currents, and multiple surface reactions.[25,32,33] However, when self-assembled monolayers (SAMs) of long linear thiol molecules are formed on the Au electrodes, the background current of the SAM-modified Au electrodes becomes significantly lower.[34–36] These properties of SAM-modified Au electrodes enable low detection limits to be obtained in electrochemical biosensors. Moreover, functionalized SAMs can be used to directly immobilize biomolecules, or to attach ligands required for biomolecule immobilization.[37,38] However, insulating SAMs of long linear thiol molecules may cause slow electron transfer between the electrode and electroactive species.[39] The moderate length of the thiol molecules can lower the background current, and also allow fast electron transfer. When SAMs are modified with a good electron mediator, such as ferrocene (Fc), the electron-transfer rate is increased.[40] If a small amount of ferrocene is tethered to SAMs of long linear thiol molecules, the background current is low but electron transfer mediated by ferrocene is rapid. In previous studies[25,40,41] we showed that a partially ferrocenyl-tethered dendrimer (Fc-D) layer exhibited such behavior.

Here we present a new redox cycling method using NADH as a reducing agent in the absence of diaphorase. The cycling was applied to an electrochemical immunosensor based on Au electrodes. First, electrochemical oxidation of NADH at SAM- and Fc-D-modified Au electrodes was investigated. AP redox cycling by NADH was then evaluated by calculating its reaction rate. Finally, an electrochemical immunosensor for mouse immunoglobulin G (IgG), using AP redox cycling by NADH, was tested and its detection limit was determined.

Experimental

Reagents

Neutravidin and 1-ethyl-3-(3-dimethylaminopropyl)carbodiimide hydrochloride (EDC) were obtained from Pierce (Rockford, USA). Amine-terminated G4 poly(amidoamine) (PAMAM) dendrimer, ferrocene carboxaldehyde, *N*-hydroxysuccinimide (NHS), mercaptododecanoic acid, mercaptoundecanol, and AP were purchased from Aldrich. Mouse immunoglobulin G (IgG) from serum, biotinylated goat antimouse IgG, alkaline phosphatase (ALP)-conjugated goat antimouse IgG, (+)-biotin *N*-hydroxysuccinimide ester (NHS-biotin), thrombin from human plasma, human prostate specific antigen (PSA), and NADH were obtained from Sigma. *p*-Aminophenylphosphate (APP) was obtained from LKT Laboratories (Saint Paul, USA). All buffer salts and other inorganic chemicals were obtained from Sigma or Aldrich, unless otherwise stated. All chemicals were used as received. Ultrapure water (> 18 MΩ, Millipore) was used in all experiments. The incubating buffer (IB) consisted of 50 mM Tris, 150 mM NaCl, and 1% BSA (pH 7.2). The rinsing buffer (RB) comprised 50 mM Tris, 0.5 M NaCl, 0.05% Tween 20, and 0.05% BSA (pH 7.5). The buffer for electrochemical experiments (EB) consisted of 50 mM Tris, 10 mM KCl, and 1 g L^{-1} $MgCl_2$ (pH 9.0).

Preparation of Fc-D

Fc-D was synthesized as previously described.[25,42] On the basis of NMR and UV/visible spectra, the extent of primary amine modification was estimated to be 0.5%.

Preparation of an immunosensing layer

Gold electrodes were prepared by electron-beam evaporation of 40 nm of Ti followed by 150 nm of Au onto Si (100) wafers. The electrode was cleaned in piranha solution [H_2O_2–H_2SO_4 (v/v) = 1 : 3], rinsed with water, and dried with N_2 gas. The cleaned electrode was immersed in a solution of 1 mM mercaptododecanoic acid and 4 mM mercaptoundecanol for 12 h, washed with pure methanol, and dried with N_2 gas. The carboxylic groups were activated by immersion of the electrode into a solution of 50 mM EDC and 25 mM NHS for 2 h, and the Fc-D solution (100 μM) was spotted onto the activated electrode and left to incubate for 2 h. Electrostatically-attached Fc-D was removed by rinsing twice with RB. To attach biotin, the Fc-D-modified electrode was immersed in a solution containing 1 mg mL^{-1} NHS-biotin for 2 h, followed by washing with methanol and water.

The biotin-modified Fc-D electrode was incubated in IB for 30 min to prevent non-specific adsorption of proteins, then washed with RB. The electrode was immersed in IB containing 100 μg mL^{-1} neutravidin for 40 min. After rinsing with RB, the resulting assembly was immersed in IB containing 100 μg mL^{-1} biotinylated goat antimouse IgG for 40 min. After washing with RB, the target mouse IgG in IB was captured by the immunosensor for 40 min, followed by washing with RB. The immunosensor was finally incubated with ALP-conjugated goat antimouse IgG for 40 min and then washed with RB.

Electrochemical experiments

The electrochemical experiment was performed using a BAS 100B electrochemical analyzer (Bioanalytical Systems, Inc.). The electrochemical cell consisted of the modified Au electrode, a Pt wire counter electrode and an Ag/AgCl reference electrode. The cell was filled with EB containing 1 mM APP and 5 mM NADH. The APP solution was prepared daily.

Results and discussion

Electrochemical oxidation of NADH at SAM- and Fc-D-modified Au electrodes

In this study we use NADH as a reducing agent for AP redox cycling. A low anodic current of NADH at the Au electrodes is required over a wide range of potentials in order to obtain low background currents. The electrochemical oxidation of NADH requires a high overpotential at the Au electrode.[28–30] However, the anodic current of NADH was considerable at the bare Au electrodes [Fig. 1(e)], and was not sufficiently low to obtain low detection limits in the electrochemical biosensor. When the Au electrodes were covered with a mixed SAM of mercaptododecanoic acid and mercaptoundecanol, the anodic

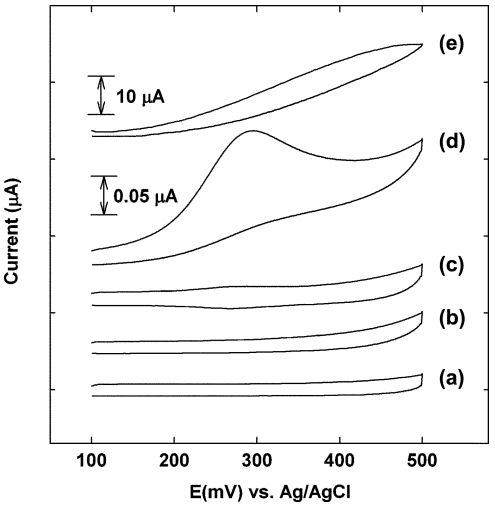

Fig. 1 Cyclic voltammograms of SAM-modified Au electrodes in (a) EB and (b) EB containing 5 mM NADH, and cyclic voltammograms of SAM- and 0.5% Fc-D-modified Au electrodes in (c) EB and (d) EB containing 5 mM NADH, and bare Au electrodes in (e) EB containing 5 mM NADH at a scan rate of 10 mV s^{-1}. The scale bars: 0.05 μA for (a)–(d), and 10 μA for (e).

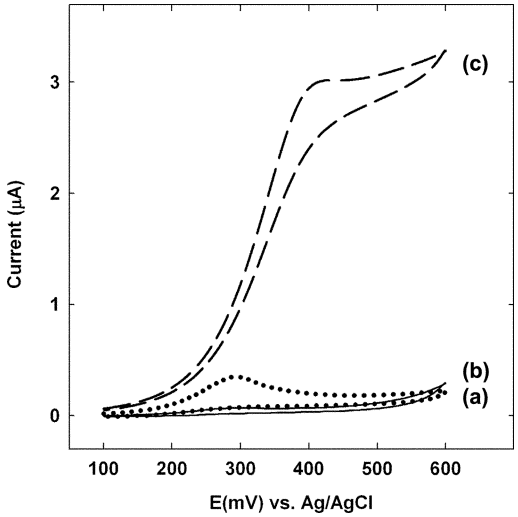

Fig. 2 Cyclic voltammograms of 0.5% Fc-D-modified Au electrodes in EB containing (a) 5 mM NADH (—), (b) 0.05 mM AP (···), or (c) both 0.05 mM AP and 5 mM NADH (---) at a scan rate of 5 mV s^{-1}.

current of NADH decreased significantly [Fig. 1(b)]. The current at 0.3 V [Fig. 1(b)] was more than 200 times lower than that at the bare Au electrodes [Fig. 1(e)], and was slightly greater than the current in the absence of NADH [Fig. 1(a)]. These results show that the anodic current of NADH was very small on the SAM-modified Au electrodes. It is likely that the dense mixed-SAM of long linear thiol molecules provided a low capacitive current and minimized unwanted electrochemical reactions. Because of the small amount of ferrocene (0.5%) in the Fc-D, we observed a small anodic peak around 0.3 V [Fig. 1(c)] at the SAM- and Fc-D-modified Au electrodes. The small amount of ferrocene enables maintenance of the low background current after Fc-D modification on the SAM-modified Au electrodes. There is a possibility that the ferrocene, which is used as a mediator for AP electro-oxidation, may mediate to electro-oxidize NADH.[26] In Fig. 1(d), an anodic current due to ferrocene-mediated NADH electro-oxidation is evident. However, the current was much less than that at the bare Au electrodes [Fig. 1(e)]. Consequently, the SAM- and Fc-D-modified Au electrodes provided a low background current, *i.e.* a low anodic current of NADH.

AP redox cycling by NADH

It is well known than AP redox cycling by diaphorase occurs in a solution containing NADH.[23] However, there has been no report of AP redox cycling by NADH. To investigate this possibility, we obtained cyclic voltammograms of AP in the absence and presence of NADH (Fig. 2). An irreversible anodic peak of AP was observed in an AP-containing solution in the absence of NADH [Fig. 2(b)]. When NADH was present, the anodic peak current was much higher [Fig. 2(c)].

Considering that the peak current in an NADH-containing solution in the absence of AP is 0.15 μA [Fig. 2(a)], the difference between the peak current in the absence (0.35 μA) [Fig. 2(b)] and presence of NADH (3 μA) [Fig. 2(c)] was not related to NADH electro-oxidation mediated by Fc-D. The enhanced peak current was mainly due to AP redox cycling by NADH. AP is oxidized to QI with the help of ferrocene at the Fc-D-modified Au electrodes. QI is reduced back to AP by NADH. Thus, generated AP is re-oxidized to QI at the Fc-D-modified Au electrodes. This redox cycling increases the anodic peak current of AP. The formal potential of an AP/QI redox couple (0.24 V *vs.* SHE at pH 7) is much more positive than that of an $NADH/NAD^+$ redox couple (–0.32 V *vs.* SHE at pH 7), which makes it possible for NADH to reduce QI to AP.

It is important to know how rapidly QI is reduced by NADH. The AP redox cycling by NADH can be regarded as an electrochemical catalytic (EC′) reaction.[31,32,43–46] The net reaction consists of one electrochemical reaction [eqn (1)] and one chemical reaction [eqn (2)].

$$AP \rightarrow QI + 2e^- \quad (1)$$

$$NADH + QI \rightarrow NAD^+ + AP + H^+ \quad (2)$$

AP is oxidized to QI by the ferrocenium ion, not by the electrode. However, the ferrocene that acts as an electron mediator is immobilized on the electrode surface, and can be regarded as electrode material. Accordingly, we express the electrochemical reaction of the EC′ reaction simply by eqn (1).

In EC′ reactions, limiting current behavior is observed at sufficiently positive potentials in cyclic voltammograms.[32] The limiting current (i_{lim}) can be represented [eqn (3)][31] by

$$i_{lim} = nFAC^*_{AP}(Dk'C^*_{NADH})^{1/2} \quad (3)$$

where k' is the rate constant of QI reduction by NADH, C^*_{AP} and C^*_{NADH} are the bulk concentrations (mol cm^{-3}) of AP and NADH, respectively, D is the diffusion coefficient of AP (6.47×10^{-6} cm^2 s^{-1}), A is the electrode area, F is the Faraday constant, and n the charge number of the electrochemical reaction.[47] With i_{lim} (3.0×10^{-6} A), A (0.283 cm^2), C^*_{AP} (0.05 mM), and C^*_{NADH} (5 mM), the calculated k' was 3.7×10^4 cm^3 mol^{-1} s^{-1}, which is similar to the value obtained in AP redox cycling by hydrazine.[25] The concentration of NADH (5 mM) was much larger than that of AP (0.05 mM). Thus, the second-order reaction can

be simplified to a pseudo-first-order reaction, and the rate is represented by:

$$\text{rate} = k'[\text{QI}][\text{NADH}] \approx k[\text{QI}] \quad (4)$$

The calculated k was 0.19 s^{-1}. The calculated half-life for the first-order reaction, (ln 2)/k, was approximately 3.7 s, which means that the concentration of QI generated by AP electro-oxidation decreases by 50% every 3.7 s.

Immunosensing using AP redox cycling by NADH

Scheme 1 is a schematic diagram of an electrochemical immunosensor using AP redox cycling by NADH, in which the target protein (mouse IgG) is captured by biotinylated antimouse IgG, and then ALP-conjugated antimouse IgG binds to the mouse IgG. The amount of bound ALP increases with the concentration of mouse IgG. To immobilize biotinylated antimouse IgG, neutravidin is pre-immobilized on Fc-D-modified Au electrodes. The low amount of ferrocene in the Fc-D layer allows a low background current along with easy oxidation of AP. ALP converts APP to AP, and after AP has accumulated for 10 min it is electro-oxidized with the help of ferrocene. AP redox cycling by NADH increases the anodic current.

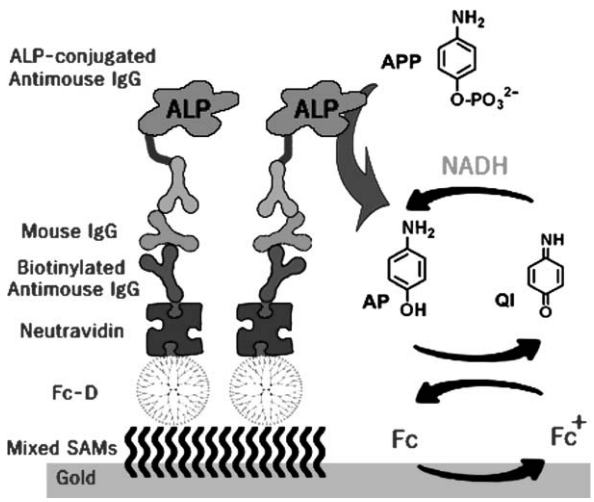

Scheme 1 Schematic illustration of a sandwich-type electrochemical immunosensor using AP redox cycling by NADH on SAM- and Fc-D-modified Au electrodes.

Cyclic voltammograms of immunosensing electrodes were obtained at various concentrations of mouse IgG in an EB solution containing 1 mM APP and 5 mM NADH (Fig. 3). We obtained at least three cyclic voltammograms at each concentration from 10 fg mL^{-1} to 10 μg mL^{-1}. The current behavior at 10 and 100 fg mL^{-1} mouse IgG was almost the same as that at 0 g mL^{-1} mouse IgG. The peak current increased with the concentration of mouse IgG from 1 pg mL^{-1}, and leveled off at concentrations over 1 μg mL^{-1}. Cyclic voltammograms obtained only at 0 g mL^{-1}, 1 pg mL^{-1}, 10 pg mL^{-1}, 100 pg mL^{-1}, 1 ng mL^{-1}, 10 ng mL^{-1}, 100 ng mL^{-1}, and 1 μg mL^{-1} mouse IgG are shown in Fig. 3.

The anodic currents at 0.4 V in the cyclic voltammograms were plotted to determine the detection limit for mouse IgG (Fig. 4). Generally, the detection limit is estimated by comparing

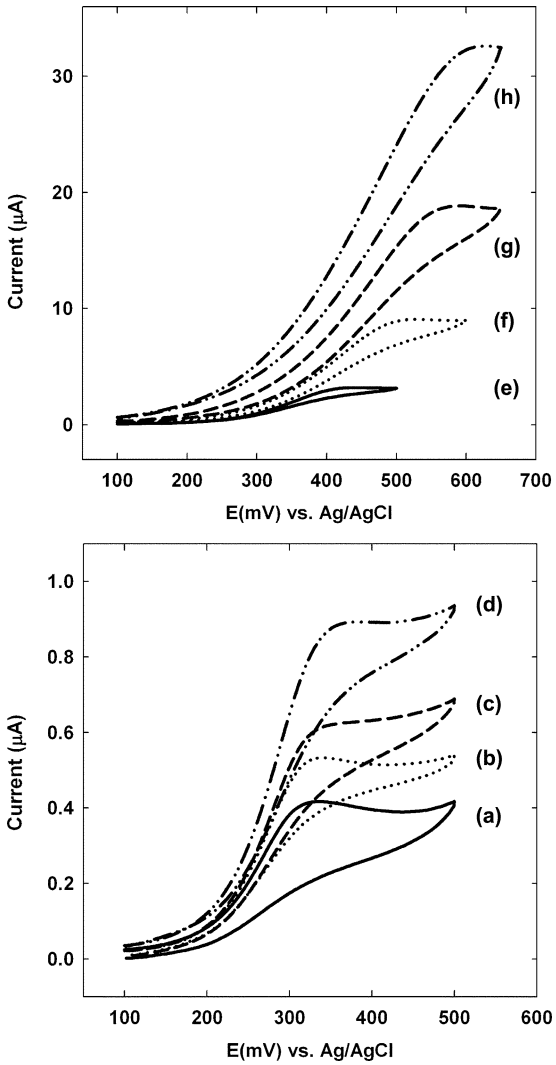

Fig. 3 Cyclic voltammograms of a sandwich-type electrochemical immunosensor for mouse IgG at various concentrations of mouse IgG: (a) 0 g mL^{-1}, (b) 1 pg mL^{-1}, (c) 10 pg mL^{-1}, (d) 100 pg mL^{-1}, (e) 1 ng mL^{-1}, (f) 10 ng mL^{-1}, (g) 100 ng mL^{-1}, and (h) 10 μg mL^{-1}. Cyclic voltammograms were obtained for 10 min after incubation in EB containing 1 mM APP and 5 mM NADH at a scan rate of 10 mV s^{-1}.

the mean current at the concentration near the detection limit with the mean current at zero concentration plus three times the standard deviation. The calculated detection limit for mouse IgG was 1 pg mL^{-1}. When NADH was not used, the detection limit was 10 pg mL^{-1} (data not shown here). The detection limit was thus reduced by one order of magnitude (from 10 to 1 pg mL^{-1}) due to AP redox cycling by NADH.

In our previous study, the detection limit of the immunosensor using 30% Fc-D-modified Au electrodes was 0.1 μg mL^{-1}.[41] In this study, however, the detection limit was 1 pg mL^{-1}, which is significantly lower because of the lower background current and redox cycling. In another previous study of ours, the detection limit for mouse IgG on 0.5% Fc-D-modified indium tin oxide (ITO) electrodes was found to be 0.1 pg mL^{-1} in the presence of hydrazine, and 10 pg mL^{-1} in the absence of hydrazine.[25] Even when redox cycling by NADH or hydrazine does not occur, low detection limits are obtained on Fc-D-modified Au

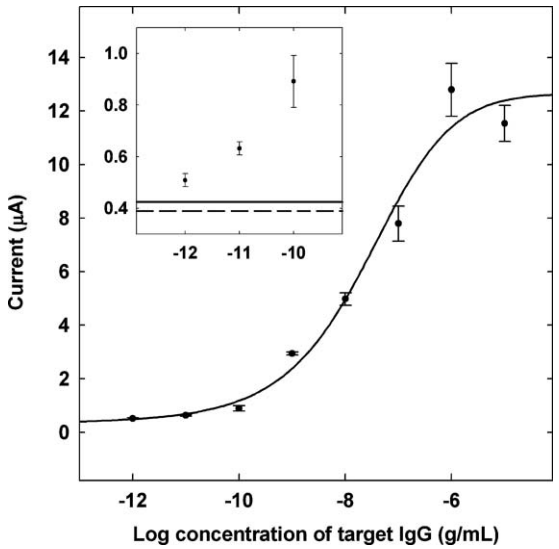

Fig. 4 Calibration plot obtained from Fig. 3. The currents at 0.3 V are taken. The dashed line represents the mean of the current obtained in 0 g mL^{-1} mouse IgG. The solid line corresponds to the mean current at the zero concentration plus three times the standard deviation (SD).

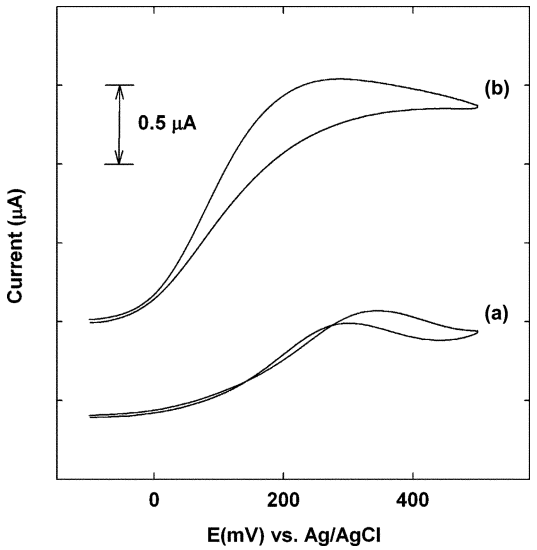

Fig. 5 Cyclic voltammograms of 5 mM hydrazine in EB at (a) the SAM-modified and (b) the 0.5% Fc-D-modified Au electrodes at a scan rate of 10 mV s^{-1}.

electrodes and Fc-D-modified ITO electrodes as a result of the low background current of both electrodes. In the case of the ITO electrodes, the low background current is mainly due to the low electrocatalytic and capacitive current of ITO itself. In the case of the Au electrodes, the background current was significantly lowered after modification of the Au electrodes with a SAM of long linear thiol molecules (Fig. 1). Thus, the SAM modification of the Au electrodes plays an important role in obtaining a low detection limit.

The rate of QI reduction by hydrazine is similar to that by NADH, and the extent of amplification by redox cycling is similar in both cases. However, the anodic current of NADH on the SAM- and Fc-D-modified Au electrodes [Fig. 1(b) and 1(d)] was much smaller than that of hydrazine [Fig. 5(a) and 5(b), respectively]. For example, the peak current in Fig. 1(d) is about one-tenth of that in Fig. 5(b). The anodic current of hydrazine was very high on the SAM- and Fc-D-modified electrodes. Although high signal amplification is obtained *via* redox cycling by hydrazine, it is not easy to acquire low detection limits on Au electrodes due to their high background current. Accordingly, it is very important to note that redox cycling by chemical was applied even to highly electrocatalytic Au electrodes because of the low background current of NADH.

To check the selectivity of our immunosensor, cyclic voltammograms were obtained in the presence of non-target proteins, PSA and thrombin (Fig. 6). The current behavior at 10 μg mL^{-1} PSA [Fig. 6(c)] and 10 μg mL^{-1} thrombin [Fig. 6(d)] is similar to that at 0 g mL^{-1} mouse IgG [Fig. 6(b)]. However, the peak current increases significantly in the presence of target mouse IgG [Fig. 6(a)]. This result shows that the sensor response is highly selective to target mouse IgG.

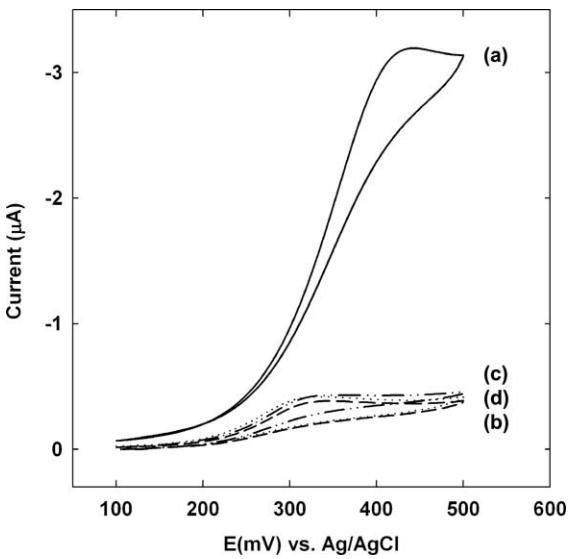

Fig. 6 Cyclic voltammograms of a sandwich-type electrochemical immunosensor for mouse IgG at (a) 1 ng mL^{-1} mouse IgG, (b) 0 g mL^{-1} mouse IgG, (c) 10 μg mL^{-1} PSA, and (d) 10 μg mL^{-1} thrombin. All cyclic voltammograms were obtained after incubating for 10 min in EB containing 1 mM APP and 5 mM NADH at a scan rate of 10 mV s^{-1}.

Conclusions

We have developed a new AP redox cycling scheme, using NADH, which can be applied to electrocatalytic Au electrodes. The Au electrodes are modified with a mixed SAM and an Fc-D layer to achieve a high signal-to-background ratio. The SAM significantly decreases the background current of the Au electrodes, and the Fc-D layer facilitates easy oxidation of AP. The low amount of ferrocene on the Au electrodes minimizes the ferrocene-mediated oxidation of NADH. The combined effect of the signal amplification by both enzymatic amplification and redox cycling, and the low background current of SAM- and Fc-D-modified Au electrodes, enabled a 1 pg mL^{-1} detection limit for mouse IgG to be achieved. This redox cycling scheme could be readily applied to all electrochemical biosensors using Au electrodes and ALP labels.

Acknowledgements

This research was supported by the Nano/Bio Science&Technology Program (2005-01333) of the Ministry of Education, Science and Technology (MEST). H. Y. acknowledges the support by the Korea Health Industry Development Institute through the Healthcare & Biotechnology Development Program (A020605).

References

1 S. Brakmann, *Angew. Chem., Int. Ed.*, 2004, **43**, 5730.
2 N. L. Rosi and C. A. Mirkin, *Chem. Rev.*, 2005, **105**, 1547.
3 L. Zhu and E. V. Anslyn, *Angew. Chem., Int. Ed.*, 2006, **45**, 1190.
4 E. D. Goluch, J. M. Nam, D. G. Georganopoulou, T. N. Chiesl, K. A. Shaikh, K. S. Ryu, A. E. Barron, C. A. Mirkin and C. Liu, *Lab Chip*, 2006, **6**, 1293.
5 J. M. Nam, S. I. Stoeva and C. A. Mirkin, *J. Am. Chem. Soc.*, 2004, **126**, 5932.
6 J. T. Mason, L. Xu, Z-m. Sheng and T. J. O'Leary, *Nat. Biotechnol.*, 2006, **24**, 555.
7 S. Hwang, E. Kim and J. Kwak, *Anal. Chem.*, 2005, **77**, 579.
8 T. Porstmann and S. T. Kiessig, *J. Immunol. Methods*, 1992, **150**, 5.
9 J. Wang, G. Liu and M. R. Jan, *J. Am. Chem. Soc.*, 2004, **126**, 3010.
10 C. A. Wijayawardhan, S. Purushothama, M. A. Cousino, H. B. Halsall and W. R. Heineman, *J. Electroanal. Chem.*, 1999, **468**, 2.
11 I. Rosen and J. Rishpon, *J. Electroanal. Chem.*, 1989, **258**, 27.
12 M. Santandreu, F. Cespedes, S. Alegret and E. M. Fabregas, *Anal. Chem.*, 1997, **69**, 2080.
13 W. R. Vandaveer IV, D. J. Woodward and I. Fritsch, *Electrochim. Acta*, 2003, **48**, 3341.
14 N. J. Forrow, N. C. Foulds, J. E. Frew and J. T. Law, *Bioconjugate Chem.*, 2004, **15**, 137.
15 S. Zhao and J. H. T. Luong, *Anal. Chim. Acta*, 1996, **327**, 235.
16 A. J. Bergren and M. D. Porter, *J. Electroanal. Chem.*, 2007, **599**, 12.
17 M. Y. Wei, L. H. Guo and H. Chen, *Microchim. Acta*, 2006, **155**, 409.
18 D. Zheng, N. Wang, F. Q. Wang, D. Dong, Y. G. Li, X. Q. Yang, L. H. Guo and J. Cheng, *Anal. Chim. Acta*, 2004, **508**, 225.
19 M. G. Ciminska, A. Holmgren, H. Andresen, K. B. Barken, M. Wumpelmann, J. Albers, R. Hintche, A. Breitenstein, P. Neubauer, M. Los, A. Czyz, G. Wegrzyn, G. Silfversparre, B. Jurgen, T. Schweder and S. O. Enfors, *Biosens. Bioelectron.*, 2004, **19**, 537.
20 J. H. Thomas, S. K. Kim, P. J. Hesketh, H. B. Halsall and W. R. Heineman, *Anal. Chem.*, 2004, **76**, 2700.
21 K. Aoki, *J. Electroanal. Chem.*, 1988, **256**, 269.
22 A. L. Ghindilis, A. Makower, C. G. Bauer, F. F. Bier and F. W. Scheller, *Anal. Chim. Acta*, 1995, **204**, 25.
23 B. Limoges, D. Marchal, F. Mavre and J.-M. Saveant, *J. Am. Chem. Soc.*, 2006, **128**, 6014.
24 J. Das, M. A. Aziz and H. Yang, *J. Am. Chem. Soc.*, 2006, **128**, 16022.
25 J. Das, K. Jo, J. W. Lee and H. Yang, *Anal. Chem.*, 2007, **79**, 2790.
26 D. Kato, S. Iijima, R. Kurita, Y. Sato, J. Jia, S. Yabuki, F. Mizutani and O. Niwa, *Biosens. Bioelectron.*, 2007, **21**, 1527.
27 H. M. Nassef, A. E. Radi and C. K. O'Sullivan, *Electrochem. Commun.*, 2006, **8**, 1719.
28 R. Antiochia, I. Lavagnini, P. Pastore and F. Magno, *Bioelectrochemistry*, 2004, **64**, 157.
29 A. Damian and S. Omanovic, *J. Mol. Catal. A: Chem.*, 2006, **253**, 222.
30 A. Kitani, Y. H. So and L. L. Miller, *J. Am. Chem. Soc.*, 1981, **103**, 7636.
31 S. Kim, S.-E. Yun and C. Kang, *J. Electroanal. Chem.*, 1999, **465**, 153.
32 A. J. Bard and L. R. Faulkner, *Electrochemial Methods: Principles and Applications*, John Wiley & Sons, New York, 2nd edn, 2001.
33 J. S. Yoo and S. M. Park, *Anal. Chem.*, 2005, **77**, 3694.
34 M. W. J. Beulen, M. I. Kastenberg, F. C. J. M. van Veggel and D. N. Reinhoudt, *Langmuir*, 1998, **14**, 7463.
35 R. E. Gyurcsanyi, A. Bereczki, G. Nagy, M. R. Neuman and E. Lindner, *Analyst*, 2002, **127**, 235.
36 Z. Liu, J. Li, S. Dong and E. Wang, *Anal. Chem.*, 1996, **68**, 2432.
37 C. D. Hodneland and M. Mrksich, *J. Am. Chem. Soc.*, 2000, **122**, 4235.
38 A. Ulman, *Chem. Rev.*, 1996, **96**, 1533.
39 F. Frederix, K. Bonroy, W. Laureyn, G. Reekmans, A. Campitelli, W. Dehaen and G. Maes, *Langmuir*, 2003, **19**, 4351.
40 E. Kim, K. Kim, H. Yang, Y. T. Kim and J. Kwak, *Anal. Chem.*, 2003, **75**, 5665.
41 S. J. Kwon, E. Kim, H. Yang and J. Kwak, *Analyst*, 2006, **131**, 402.
42 H. C. Yoon, M.-Y. Hong and H.-S. Kim, *Anal. Chem.*, 2000, **72**, 4420.
43 L. A. Coury, Jr., R. W. Murray, J. L. Johnson and K. V. Rajagopalan, *J. Phys. Chem.*, 1991, **95**, 6034.
44 L. A. Coury, Jr., B. N. Oliver, J. O. Egekeze, C. S. Sosnoff, J. C. Brumfield, R. P. Buck and R. W. Murray, *Anal. Chem.*, 1990, **62**, 452.
45 M. D. Gonzalez, M. B. C. Garcia and A. C. Garcia, *Electroanalysis*, 2005, **17**, 1901.
46 A. Warsinke, A. Benkert and F. W. Scheller, *Fresenius' J. Anal. Chem.*, 2002, **66**, 622.
47 D. Robinson, J. E. Anderson and J. L. Lin, *J. Phys. Chem.*, 1990, **94**, 1003.

